Evaluation of a New Carbon Dioxide System for Autonomous Surface Vehicles

CHRISTOPHER SABINE,[a] ADRIENNE SUTTON,[b] KELLY MCCABE,[c] NOAH LAWRENCE-SLAVAS,[b] SIMONE ALIN,[b] RICHARD FEELY,[b] RICHARD JENKINS,[d] STACY MAENNER,[b] CHRISTIAN MEINIG,[b] JESSE THOMAS,[e] ERIK VAN OOIJEN,[f] ABE PASSMORE,[f] AND BRONTE TILBROOK[f]

[a] *University of Hawai'i at Mānoa, Honolulu, Hawaii*
[b] *NOAA/Pacific Marine Environmental Laboratory, Seattle, Washington*
[c] *University of South Carolina, Columbia, South Carolina*
[d] *Saildrone, Inc., Alameda, California*
[e] *Liquid Robotics, Inc., Sunnyvale, California*
[f] *Commonwealth Scientific and Industrial Research Organisation, Hobart, Tasmania, Australia*

(Manuscript received 29 January 2020, in final form 29 May 2020)

ABSTRACT

Current carbon measurement strategies leave spatiotemporal gaps that hinder the scientific understanding of the oceanic carbon biogeochemical cycle. Data products and models are subject to bias because they rely on data that inadequately capture mesoscale spatiotemporal (kilometers and days to weeks) changes. High-resolution measurement strategies need to be implemented to adequately evaluate the global ocean carbon cycle. To augment the spatial and temporal coverage of ocean–atmosphere carbon measurements, an Autonomous Surface Vehicle CO_2 ($ASVCO_2$) system was developed. From 2011 to 2018, $ASVCO_2$ systems were deployed on seven Wave Glider and Saildrone missions along the U.S. Pacific and Australia's Tasmanian coastlines and in the tropical Pacific Ocean to evaluate the viability of the sensors and their applicability to carbon cycle research. Here we illustrate that the $ASVCO_2$ systems are capable of long-term oceanic deployment and robust collection of air and seawater pCO_2 within ± 2 μatm based on comparisons with established shipboard underway systems, with previously described Moored Autonomous pCO_2 ($MAPCO_2$) systems, and with companion $ASVCO_2$ systems deployed side by side.

1. Introduction

As a carbon sink, the oceans have helped buffer climate change during the Anthropocene by absorbing approximately one-quarter of the carbon dioxide (CO_2) emitted to the atmosphere from human activity (Friedlingstein et al. 2019; Gruber et al. 2019; Sabine et al. 2004). Indeed, measurements of surface waters are documenting the fact that although much more variable than the atmosphere, over long time and space scales the ocean CO_2 levels are increasing at about the same rate as the atmospheric CO_2 concentrations (Bates et al. 2014; Landschützer et al. 2014; Takahashi et al. 2009; Wanninkhof et al. 2013a). The oceanic removal of CO_2 from the atmosphere is reducing the effects of climate change but in turn it is acidifying surface seawater.

The ocean removes carbon from the atmosphere via gas equilibration and moves it into the ocean interior at deep and intermediate water formation regions, in a process known as the solubility pump. Atmospheric carbon dioxide is also moved into the ocean interior via the biological pump, when the carbon that is taken up by phytoplankton during photosynthesis is transported down as organisms die or are eaten and repackaged into fecal pellets. Much of this biologically fixed organic carbon sinks to the subsurface ocean, where it is rapidly remineralized or respired back to dissolved CO_2. Because both of the solubility and biological pumps vary by region and season, there is tremendous spatial and temporal variations in surface ocean CO_2 concentrations (Bates et al. 2014; Landschützer et al. 2014; Takahashi et al. 2009; Wanninkhof et al. 2013a).

Coastal regions are particularly vulnerable to changes in ocean carbon chemistry and its biological impacts.

Denotes content that is immediately available upon publication as open access.

Corresponding author: Christopher Sabine; csabine@hawaii.edu

DOI: 10.1175/JTECH-D-20-0010.1

Changes in tides, temperature, salinity, and primary production expose coastal regions to seasonal and spatial variations in surface ocean dissolved CO_2 concentrations (Bauer et al. 2013; Damm et al. 2010; Fassbender et al. 2018). For example, along the Pacific coast of the United States, seasonal (late spring to early fall) strengthening of the northwesterly winds transport dense, CO_2-rich water from the subsurface up onto the continental shelf, exposing coastal ecosystems to potential acidification from both natural and anthropogenic sources (Fassbender et al. 2018; Feely et al. 2016). Changes in the frequency, duration, and intensity of acidified conditions will affect marine ecosystems in ways that we are only starting to understand (Barton et al. 2012; Bednaršek et al. 2012, 2014a,b, 2017; Fabry et al. 2008; Kleypas et al. 2006; Reum et al. 2015). The fate of these economically important regions is still largely unknown due to the limitations of applying results of laboratory experiments to the complexity of real-world ecosystems, as well as a paucity in current biological and carbon system monitoring approaches.

Underway systems on research ships and commercial volunteer observing ships as well as autonomous systems on mooring platforms have documented substantial variations in the oceanic partial pressure of CO_2 (pCO_2) and subsequent carbonate chemistry of coastal waters (Fassbender et al. 2018; Feely et al. 2016; Sutton et al. 2019; Wanninkhof et al. 2015). While research expeditions can gather data over vast spatial scales, large-scale coastal expeditions occur infrequently. This fails to capture mesoscale temporal (days to weeks) variations in the carbon cycle. Mooring deployments compensate for the temporal gaps by capturing high-frequency time series, but the sparsity of moorings that measure CO_2 leaves large spatial gaps. Spatiotemporal gaps left by current measurement strategies hinder the scientific understanding of the oceanic carbon cycle, especially in coastal regions that are exposed to mesoscale physical and biogeochemical forcing.

Much of the carbon data collected from ships (bottle measurements and underway pCO_2 systems) and moored platforms have been synthesized into data products. Data products such as the Lamont Doherty Earth Observatory surface ocean pCO_2 database (Takahashi et al. 2009), the Surface Ocean CO_2 Atlas (SOCAT) (Bakker et al. 2016) and the Global Data Analysis Project (GLODAP) (Olsen et al. 2019) provide the basis for ocean uptake calculations and validation of model simulations (Gruber et al. 2019; Wanninkhof et al. 2013b). Together, large-scale carbon data products and modeling efforts have improved our understanding of oceanic carbon cycling and allowed for better climate predictions. Unfortunately, large-scale and global data products and models are subject to regional bias because they rely on data that inadequately capture mesoscale spatiotemporal (kilometers and days to weeks) changes. High-resolution spatiotemporal measurement strategies need to be implemented in order to adequately evaluate the regional aspects of the global ocean carbon cycle.

To augment the spatial and temporal coverage of ocean–atmosphere carbon measurements, the National Oceanic and Atmospheric Administration (NOAA) Pacific Marine Environmental Laboratory (PMEL) developed an Autonomous Surface Vehicle CO_2 ($ASVCO_2$) system for deployment on remotely operated autonomous platforms. In collaboration with Liquid Robotics Inc. (liquid-robotics.com) and Saildrone Inc. (saildrone.com), PMEL integrated $ASVCO_2$ systems (Fig. 1) on two types of autonomous surface vehicles, a Wave Glider and Saildrone. Similar pCO_2 instruments have been deployed on Wave Gliders recently (Chavez et al. 2018; Northcott et al. 2019), but the $ASVCO_2$ system has the advantage of being directly comparable to a network of moored CO_2 systems deployed in all the major ocean basins. The $ASVCO_2$ systems described here were deployed on four Wave Glider and three Saildrone missions along the U.S. Pacific coast, Australia's Tasmanian coastline, and in the tropical Pacific between 2011 and 2018 in order to evaluate the performance of the sensors, and the utility of these systems in carbon cycle research.

2. Methods

a. *$ASVCO_2$ system*

The $ASVCO_2$ system is a modified version of the Moored Autonomous pCO_2 ($MAPCO_2$) system developed by PMEL and Monterey Bay Aquarium Research Institute, which has been used for over a decade on dozens of moored surface buoys around the world (Sutton et al. 2014). The details of the $ASVCO_2$ design, components (including equilibrator design), gas flow paths, and analysis sequences/timing are all identical to the $MAPCO_2$ except as noted here, so they will not be repeated. The modifications primarily involved a repackaging of the components and the development of small, high pressure gas bottles for the reference gas (Luxfer M22A high pressure carbon wrapped, aluminum-lined cylinder) for deployment on the Liquid Robotics, Inc., Wave Glider (Willcox et al. 2010) and Saildrone, Inc. (Meinig et al. 2015), surface vehicles. The new cylinders were extensively tested at NOAA's Earth System Research Laboratory for more than a year to ensure the concentrations did not significantly drift (<0.1 ppm over six months) before they were implemented. A manifold linking three small bottles together along with a lower flow rate (from 0.25 LPM on $MAPCO_2$ to

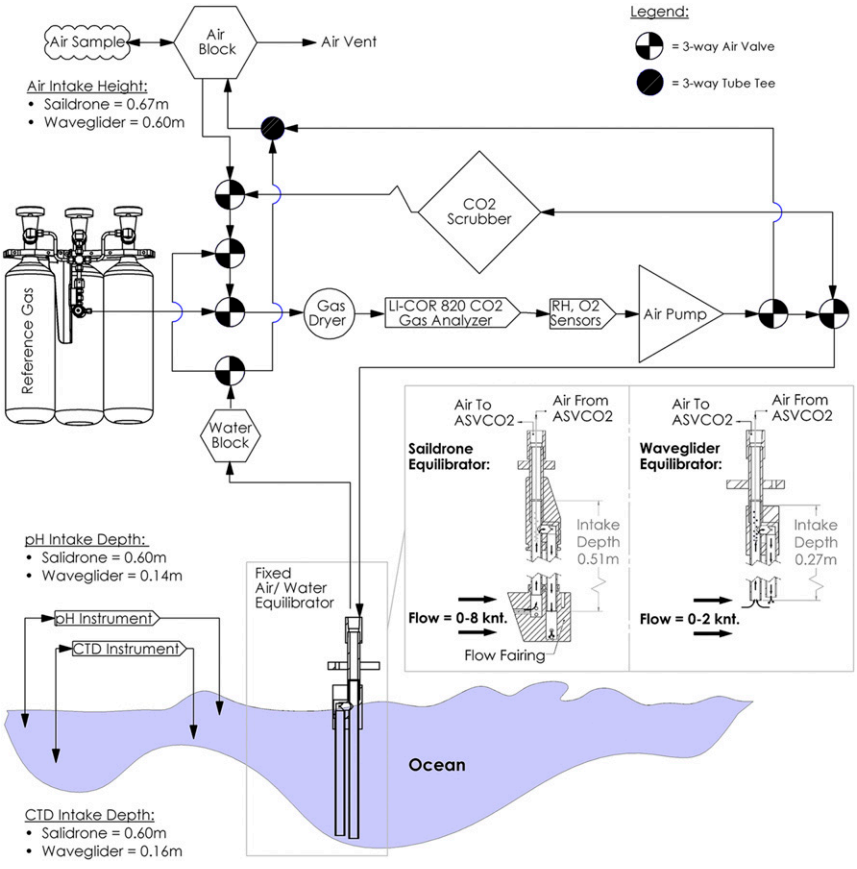

FIG. 1. $ASVCO_2$ system components and sampling paths.

0.13 LPM on $ASVCO_2$) was used for long deployments (Fig. 1). The equilibrator was shortened and placed at a fixed depth compared to the floating equilibrators used on the buoy-based $MAPCO_2$ systems, with the Wave Glider and Saildrone acting as the float. The equilibrator operated on the same bubble equilibration principles as described by Sutton et al. (2014). A fairing was added on the equilibrator water inlet and exit of the Saildrone system to prevent both sucking all the water out of the equilibrator and filling the equilibrator with water when moving at higher speeds of 4 + kt ($1\,kt \approx 0.51\,m\,s^{-1}$).

Like the $MAPCO_2$ system, the primary measurement was made using a nondispersive infrared (NDIR) detector (Li-Cor-820) either on air drawn from the atmosphere above the vehicle (0.6 m above sea level for Wave Glider or 0.7 m for Saildrone) or on air equilibrated with surface seawater. The gas streams were partially dried by passing through a 0.14 m Nafion tube packed in silica desiccant. The Li-Cor was calibrated before every set of atmospheric and seawater-equilibrated air measurements using a closed loop of air drawn through a soda lime column (~35 g) to scrub out all CO_2 to zero the instrument, then using a gas with a known CO_2 concentration (traceable to the World Meteorological Organization and supplied by NOAA's Earth System Research Laboratory) to span it. Detector calibration shows a precision and accuracy comparable to the mooring-based systems (<0.7 and <1.5 μatm, respectively; Sutton et al. 2014). Measurements can be made on approximately 30-min intervals; however, measurements were typically made at hourly intervals on field deployments. The mole fraction of air CO_2 (xCO_2) equilibrated with surface seawater was determined using temperature and relative humidity, and pCO_2 was subsequently calculated by multiplying the xCO_2 by total pressure (Sutton et al. 2014). An internal GPS recorded the position and time of each measurement.

A Honeywell Durafet III ion-sensitive field-effect transistor (ISFET) pH sensor (Martz et al. 2010) was also fixed within the $ASVCO_2$ waterproof enclosure (Fig. 1). The Durafet response time is milliseconds, but readings were averaged over the same time period that the CO_2 measurements were collected. For deployment on the Wave Glider, the sensor was directly exposed to the surrounding water. On the Saildrone, the instrument

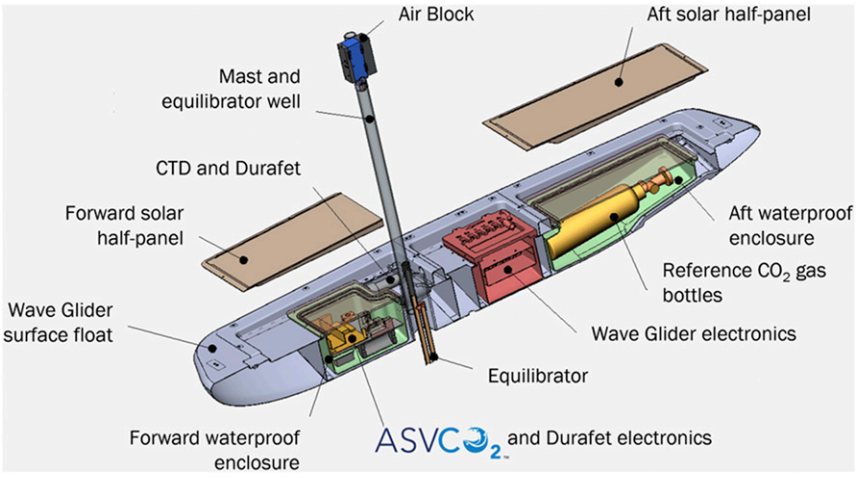

FIG. 2. Cross section of the Liquid Robotics, Inc., Wave Glider surface float with the ASVCO$_2$ system. Various configurations of reference CO_2 gas bottles have been tested; here we show one gas cylinder, and Fig. 1 shows three.

was inside a housing with surface water pumped through antifoulant to reduce biofouling. The Durafet has a laboratory-based reported short-term (order of hours) precision of ±0.0005 pH units that weakens to approximately ±0.005 pH units over longer periods (order from weeks to months) (Martz et al. 2010). Accuracy was assessed in situ using independent validation data (Bresnahan et al. 2014).

A Sea-Bird Scientific Prawler CTD (SBE37 variant) measured sea surface temperature (SST) and sea surface salinity (SSS) simultaneously with the pair of carbon parameters, pCO_2 and pH. In addition, an SBE63 dissolved oxygen sensor was used on the Wave Glider. For the Saildrone, an Aandera 4831 dissolved oxygen sensor was located in the pumped and poisoned housing with the pH. An oxygen sensor is also part of ASVCO$_2$ gas analysis, but that is primarily for diagnostics and does not replace the in situ sensor. All measurements were recorded on approximately 30-min or hourly intervals and saved to the internal memory card. While integration of pH and dissolved oxygen sensors into the ASVs are introduced here, the field evaluation of data quality focuses on air–sea CO_2 measurements made by the PMEL-built ASVCO$_2$.

b. *Autonomous vehicle platforms*

The ASVCO$_2$ system was integrated into both the Wave Glider and Saildrone autonomous surface vehicles. The Liquid Robotics Inc. Wave Glider SV2 float is 210 cm × 60 cm ($L \times W$). The float joins submerged articulated fins (191 cm × 40 cm) with a 4-m tether. The articulated fins harness wave energy below the float to propel the platform forward through the water with an average speed of 1.1 kt (Willcox et al. 2010). Two solar panels sit atop the float and harvest sunlight (a maximum of 112 W) to charge the battery (maximum payload of 40 W) that powers the sensors. The Wave Glider's ability to harness solar and wave energy as well as the programmable course feature allows it to operate at sea for several months at a time without servicing. The programmable course can be modified by a land-based pilot through an Iridium satellite communication link. Other mobility features include targeted station keeping and repetitive course holding. Averaged data were returned to shore in real time via the Iridium satellite communication link and raw data saved on the memory flash card.

The ASVCO$_2$ electronics and pH sensor were modified to fit in a custom form waterproof box that was secured near the front of the float. The equilibrator and air block were mounted in the center of the float. The span gas bottles were located in the rear end of the float (Fig. 2). The CTD was mounted just aft of the equilibrator at 0.3-m depth. Although the ASVCO$_2$ system was tested on the Liquid Robotics, Inc., Wave Glider SV2 model, introduced in 2008, the ASVCO$_2$ system's versatile design can easily be integrated onto the new, larger, faster SV3 model introduced in 2013 and the variants added in 2017 and 2019.

The Saildrone is a wind-powered autonomous surface vehicle with a 7-m hull, 5-m wing sail, and 2.5-m keel (Fig. 3). It has an average speed of ~3 kt but can reach speeds of up to 8 kt. Solar panels and batteries provide power to the onboard electronics and instruments. A number of scientific instruments have been integrated into the vehicle over the last decade, including the ASVCO$_2$ system (Meinig et al. 2015, 2019). The ASVCO$_2$ system was packaged in a manner similar to

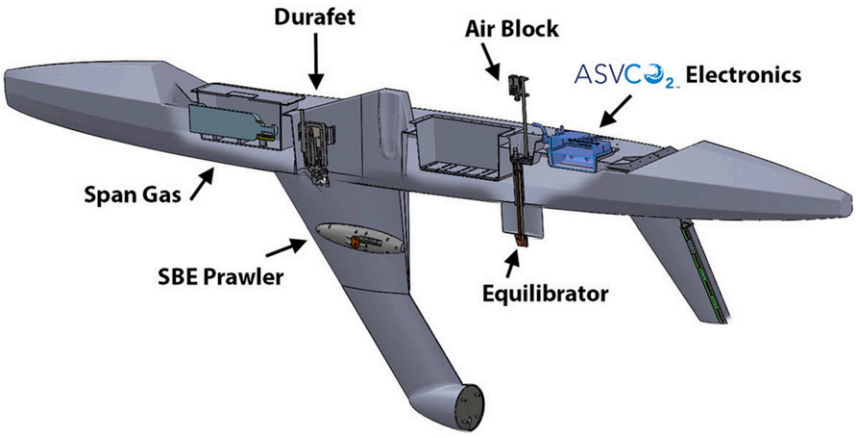

FIG. 3. Cross section of the Saildrone with the integrated $ASVCO_2$ system and associated components.

the Wave Glider, except for the air and water intake levels, pH mounting, and dissolved oxygen sensor used as noted in section 2a. The CTD was mounted in a tunnel inside the keel at 0.5-m depth. The pH sensor was housed in the hull near the $ASVCO_2$ system in a channel pumped through antifoulant.

As with the Wave Glider, the Saildrone can be autonomously controlled from shore via Iridium satellite communications. To ensure safe operations at sea, both the Wave Glider and Saildrone carry automated identification system (AIS) transceivers, enabling them to see surrounding commercial traffic. Raw data were stored on board, and averaged data were transmitted to shore in near–real time. To assess data quality, the $ASVCO_2$ systems integrated on both carbon Wave Gliders and Saildrones were deployed off the U.S. Pacific coast from 2011 to 2018 and on Saildrones deployed off Australia's Tasmanian coast in 2018 (see Fig. 4). All data are available through the National Centers for Environmental Information (www.ncei.noaa.gov) and

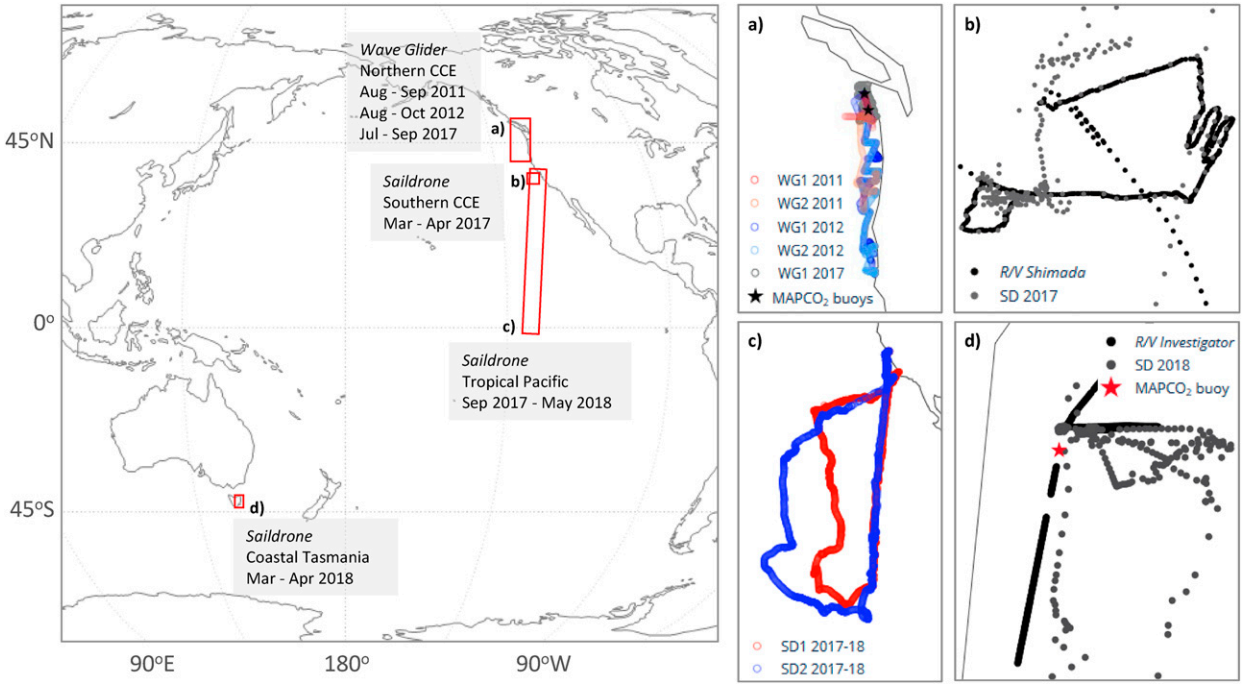

FIG. 4. (left) Locations and mission dates for the Wave Glider and the Saildrone $ASVCO_2$ deployments. Insets show (a) Wave Glider deployments in the northern California Current ecosystem (CCE), (b) ship and Saildrone intercomparison in the southern CCE, (c) Saildrone deployment to the tropical Pacific, and (d) Saildrone intercomparison in coastal Tasmania.

SOCAT (www.socat.info), except for the data collected in Tasmanian coastal waters, which are available through the Integrated Marine Observing System (http://imos.org.au/) and SOCAT.

c. Deployments

1) Wave Glider

The locations and mission dates for all $ASVCO_2$ deployments presented here are shown in Fig. 4. On 4 August 2011 two Wave Glider vehicles were deployed off of Washington State using the 10-m Washington Department of Fish and Wildlife (WDFW) vessel, R/V *Corliss* (Fig. 4a). One Wave Glider occupied a zonal track along 47.1°N between 125.2° and 124.7°W. The National Data Buoy Center's Cape Elizabeth mooring, which was outfitted with a $MAPCO_2$ system, was on the primary zonal line. The Wave Glider made 14 passes around the mooring. It also made one excursion to the north to make a pass around the University of Washington's La Push/*Ćháʔba* (Quileute for "whale tail") mooring, which was also outfitted with a $MAPCO_2$ system, before it was recovered on 29 September 2011.

The second Wave Glider traveled along the same zonal path for a week before transitioning south to transit longitudinally along the Washington and Oregon coastlines. Both Wave Gliders were brought back together off the Washington coast for recovery after nearly two months of operation. The following year the same two Wave Glider/$ASVCO_2$ systems were deployed off of Washington State with a mission of surveying the coastal upwelling system along the U.S. West Coast. They were deployed on 23 August 2012 from the WDFW vessel, the R/V *Corliss*, just west of the harbor off of Westport, Washington. Both Wave Gliders traveled south in a zigzag pattern down to Eureka, California (~25°W from 48° to 40.8°N), with one vehicle leading and the second following the same path eight days later. Once the Wave Gliders reached Eureka, they were recovered, shipped back to Washington, and deployed again 6 days later to repeat the track. The final recovery was on 18 October 2012.

In 2017, one Wave Glider with an $ASVCO_2$ system was deployed again off the Washington State coast to survey coastal waters in the northern California Current System during the upwelling season (Fig. 4a). This deployment started earlier in the season compared to the 2012 mission and surveyed a coastal area north of the region surveyed during the 2012 mission. The full 2017 mission was from 27 July to 27 September 2017. The Wave Glider was deployed and recovered from the Olympic Coast National Marine Sanctuary vessel the R/V *Tatoosh* near the La Push/*Ćháʔba* buoy at 48.0°N, 125°W. After deployment, the Wave Glider traveled south in a zigzag pattern down to 46.9°N just west of Westport, then returned north following the same pattern. $ASVCO_2$ systems have also been deployed on Wave Gliders in the Bering Sea, Chukchi Sea, Gulf of Alaska, South Central Pacific, and Southern Ocean; however, quality-controlled data are not yet available for high-quality intercomparisons.

2) Saildrone

A couple of months before the last Wave Glider mission, the first field intercomparison of the $ASVCO_2$ system on a Saildrone was conducted (Fig. 4b). The intercomparison period had a duration of approximately 24 h from 21 to 22 March 2017 and was carried out in coastal waters just south of San Francisco Bay and approximately 20 n mi (1 n mi = 1.852 km) offshore. The Saildrone sailed from Saildrone Inc. headquarters in Alameda, California to the testing site where it rendezvoused with the R/V *Shimada*. The purpose of the deployment was to allow for a field intercomparison between instruments deployed on the Saildrone to those aboard the R/V *Shimada*, including a General Oceanics 8050 underway pCO_2 system (Pierrot et al. 2009). The first activity was a box grid, followed by a straight-leg transit headed east from the box grid, then a series of transects set out in a zigzag pattern, and finally another transect with an L shape headed first north and then west (Fig. 4b). The R/V *Shimada* was generally within about 600 m of the Saildrone and at times less than 200 m, especially for the straight transect headed west. After the intercomparison with the ship, the Saildrone headed south to the CCE1 buoy located at 33.5°N, 122.5°W for an intercomparison with the $MAPCO_2$ system. From 19 to 25 April, the Saildrone sailed a box around the buoy generally within less than 1 km of the buoy. After this intercomparison, the Saildrone returned to Alameda.

On 1 September 2017, two Saildrones with $ASVCO_2$ systems departed Alameda for the tropical Pacific (Fig. 4c). While intercomparisons with $MAPCO_2$ systems on buoys were planned, low wind conditions prevented the Saildrone from safely navigating near the buoys. However, during the three months that both Saildrone $ASVCO_2$ systems made CO_2 measurements, the vehicles sailed together to allow for comparisons between the two systems. After traveling as far south as 3°S, both Saildrones returned north and were recovered off the central California coast in early May 2018.

On 28 March 2018 three Saildrones with $ASVCO_2$ systems departed Hobart, Tasmania, Australia, for a field intercomparison with air and surface water measurements made on the R/V *Investigator* and a $MAPCO_2$ system on the mooring on located at 42.7°S, 148.2°E to the

TABLE 1. Statistical comparison of ASVCO$_2$ xCO$_2$ (μmol mol^{-1}) measurements minus concurrent measurements made by moored MAPCO$_2$ systems, ship underway CO$_2$ systems, and another ASVCO$_2$ system. Comparisons include all data when both platforms were within 1 km and measurements were within 20 min. Sample size n, mean, and 1 standard deviation of the mean are shown for each platform–platform comparison and all comparisons combined for air and seawater xCO$_2$.

	Atmospheric xCO$_2$ (μmol mol^{-1})			Seawater xCO$_2$ (μmol mol^{-1})		
	n	Mean	Std dev	n	Mean	Std dev
MAPCO$_2$ vs ASVCO$_2$	83	0.4	2.7	82	1.2	6.9
Underway vs ASVCO$_2$	23	1.1	0.9	56	−1.2	3.0
ASVCO$_2$ vs ASVCO$_2$	209	0.1	1.3	112	−1.4	3.4
All comparison data	315	0.3	2.0	250	−0.5	4.9

east of Maria Island, Tasmania (Fig. 4d). Air measurements on the R/V *Investigator* were recorded as 1-min averages of 22 readings using a Picarro 2301 cavity ring-down spectrometer (Humphries et al. 2019) as part of the Global Atmosphere Watch program of the World Meteorological Organization. Surface water measurements were made using a General Oceanics 8050 underway pCO$_2$ system. Starting on 3 April, the Saildrones spent 36 h navigating a box grid around the Maria Island buoy, then transited east to meet the R/V *Investigator* for an intercomparison starting on 5 April. The Saildrones held a steady course for about 6 h separated from each other by about 300 m and the ship trailing behind the Saildrones by about 300–600 m. After this intercomparison, two Saildrones returned to the Maria Island buoy, while one continued south to test Saildrone performance in Southern Ocean conditions. ASVCO$_2$ systems have also been deployed on Saildrones in the Bering Sea, Chukchi Sea, and Southern Ocean; however, quality-controlled data are not yet available for high-quality intercomparisons.

d. Data quality assurance and control

Prior to all deployments, the ASVCO$_2$ systems were run in a laboratory test tank and compared with MAPCO$_2$ and a General Oceanics 8050 underway CO$_2$ systems as described in more detail by Sutton et al. (2014). The test tank was used to ensure that the systems were running properly and CO$_2$ values were within specifications (±2 ppm) of the comparison systems with known data quality.

During the field deployment, the systems sent back summary data, including a range of diagnostic information, once per day so the system operation could be evaluated. Diagnostic information (e.g., internal pressures with air pumps on and off, calibration flags, and relative humidity) provide information on any flow restrictions or mechanical problems with the air handling and Li-Cor operation.

Once the vehicles were recovered, the raw data were downloaded from the systems and processed in the same manner described by Sutton et al. (2014) for the MAPCO$_2$ systems. Quality control program flags were assigned following WOCE guidelines: flag of 2 (good), 3 (questionable), and 4 (bad). Any data flagged as bad were excluded from the plots and intercomparisons shown here. Questionable flags, often caused by diagnostic issues, were individually evaluated. If the data were flagged because of a non-CO$_2$ related issue, then they were included in the analyses.

Data quality was evaluated from the diagnostic information collected with the measurements, through a comparison of air CO$_2$ values with the NOAA Greenhouse Gas Marine Boundary Layer Reference (Dlugokencky et al. 2016) from the same time period and latitude, and through comparisons of CO$_2$ values against MAPCO$_2$ moorings or shipboard underway measurements (Table 1).

One difficulty with water pCO$_2$ comparisons is the small time and space scales of variability. In the field it is difficult to determine if differences between systems reflect errors in the measurements or real variations between the sampling times and locations. Comparisons between systems were generally restricted to times within 20 min and 1 km of each. As the differences generally increased with separation distance, the comparisons clearly include both the analytical errors and real variability.

3. Results and discussion

a. Carbon sensor verification

One way to evaluate the system performance while deployed is to look at the calibration results. The system calibrates itself before every set of measurements, but readings of the zero air and the span gas are made immediately before the calibration. By comparing the zero reading before and after the calibration, a sense of the instrumental stability can be determined. The standard deviation of all zero air calibrations during the deployments described here was 0.7 μmol mol^{-1}, the same as the reported xCO$_2$ precision determined in the laboratory

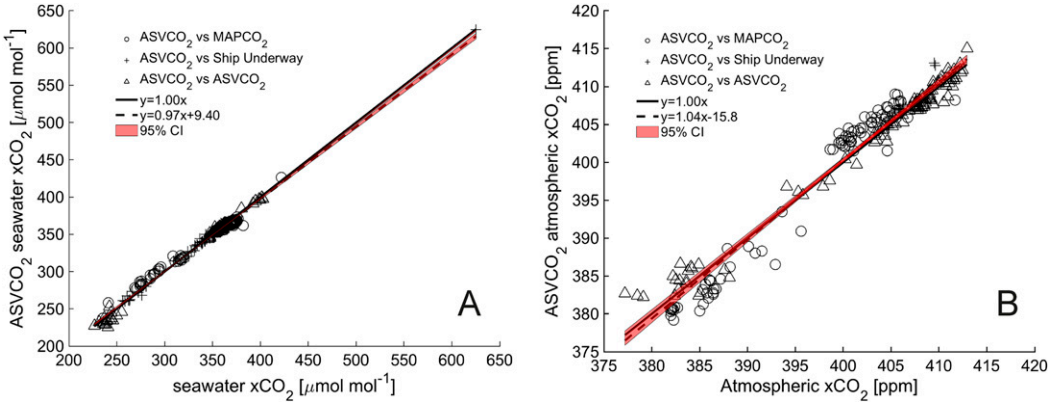

FIG. 5. Comparison of $ASVCO_2$ (a) seawater and (b) atmospheric measurements with concurrent measurements (within 20 min) made on a ship's underway CO_2 system (crosses), from moored buoys (circles), or from another $ASVCO_2$ system (triangles) while within 1 km of an $ASVCO_2$ system. The $ASVCO_2$ seawater measurements are in good agreement with both of the other platform measurements over the range of measured values as shown by the strong (both $R^2 = 0.99$; RMSE = 4.82 and 4.66, respectively) positive ~1:1 linear (both slopes ~1) relationship. The atmospheric CO_2 comparison data show a similar strong (both $R^2 = 0.96$; RMSE = 1.97 and 1.94, respectively) positive linear relationship (both slopes ~1). These results further support the accuracy and precision of the $ASVCO_2$ system detailed in Table 1.

and consistent with the reported $MAPCO_2$ precision (Sutton et al. 2014).

The span gas adjustments before and after calibration were up to two orders of magnitude larger than the zero adjustments. This is not surprising because the NDIR CO_2 signal is a strong function of temperature and pressure. Thus, the environmental effects are much more prevalent at higher CO_2 concentrations. Although temperature and pressure are measured in the NDIR detector, small variations in environmental conditions can impact the calibration. This is exactly why the system is calibrated immediately before every measurement, so the calibration is at the same environmental conditions as the in situ measurements.

1) ATMOSPHERIC CARBON DIOXIDE

Atmospheric CO_2 comparisons in offshore conditions provide a good test of system performance because the atmosphere is relatively well mixed and variations in time and space are significantly smaller than in the ocean. Average atmospheric xCO_2 ($xCO_{2,atm}$) concentrations recorded along the U.S. West Coast of 384.6 ± 6.7 ppm (or μmol mol^{-1}) from August to September 2011, 390.0 ± 5.3 ppm from July to October 2012, and 402.7 ± 8.6 ppm from July to September 2017 agree with the Mauna Loa Observatory Northern Hemisphere monthly in situ $pCO_{2,atm}$ mean values of 389.6, 392.3, and 406.6 ppm, respectively (Dlugokencky et al. 2019; Keeling et al. 2005). The average $xCO_{2,atm}$ concentration recorded along Australia's Tasmanian coast in 2018 of 404.3 ± 2.0 ppm compares well with the flask $pCO_{2,atm}$ monthly average of 403.3 ppm measured at Baring Head, New Zealand (Dlugokencky et al. 2019; Keeling et al. 2005).

Comparisons of $xCO_{2,atm}$ with underway and mooring systems (within 20 min, and within 1 km) showed more variability than the $xCO_{2,atm}$ comparisons with the flask sampling, with values spiking as high as 415 ppm (Fig. 5b). Part of that variability may be explained by the proximity to shore or another local source of elevated atmospheric CO_2. Many of these measurements were made in coastal regions where offshore winds can introduce elevated CO_2 (Lindquist et al. 2018).

To reduce as much variability between the comparison platforms as possible, Table 1 shows comparisons when platforms measured within 20 min and 1 km. Based on 83 comparisons between the $ASVCO_2$ system and buoy-mounted $MAPCO_2$ systems, there was no significant bias in atmospheric xCO_2 and a mean difference of 0.4 ± 2.7 ppm (mean ± 1 standard deviation). There were 23 comparisons between shipboard underway measurements and the $ASVCO_2$ system. The $ASVCO_2$ measurements were on average 1.1 ppm higher than the underway system with a mean difference of 1.1 ± 0.9 ppm. Comparisons with shipboard measurements can be a challenge because the ship's air intake can be higher than the $ASVCO_2$ system, there can be contamination from the ship as the air is transported to the underway system, and the ship's engines are a large local source of CO_2, that either the underway or the autonomous systems may detect.

Because both the autonomous platforms and the instrumental systems are new technologies, they were typically deployed in pairs. This allowed a more thorough

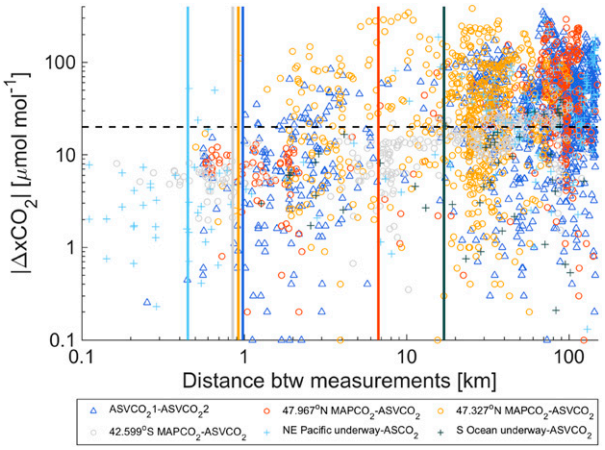

FIG. 6. The absolute difference between $ASVCO_2$ seawater measurements and concurrent seawater measurements (within 20 min) made by ship underway systems (light blue and gray crosses), moored buoys (orange, yellow, and light-gray circles) or another $ASVCO_2$ system (blue triangles) as a function of distance between the two platforms.

evaluation of total system performance as the two systems could be compared with each other under a variety of conditions. There were 209 opportunities to compare simultaneous atmospheric CO_2 measurements made from two independent $ASVCO_2$ systems within 1 km of each other. These comparisons showed a mean difference of 0.1 ± 1.3 ppm.

The comparison for all deployments and platforms showed an overall mean difference of 0.3 ± 2.0 ppm (Table 1). Figure 5b further shows the agreement between $xCO_{2,atm}$ measured on the new $ASVCO_2$ system and other platforms (slope ≈ 1; $R^2 > 0.96$; RMSE < 2). The data were carefully examined to look for biases associated with a particular platform, time of year, or geographical location. No significant trends or biases were found.

2) SURFACE WATER CARBON DIOXIDE

As noted previously, comparisons of the surface seawater xCO_2 measurements can be more difficult to interpret given the greater dynamic range and slower mixing. Figure 6 shows the absolute difference between an $ASVCO_2$ system and either another $ASVCO_2$ system, a buoy based $MAPCO_2$ system, or a shipboard underway CO_2 system as a function of distance between the two platforms. The differences generally increase as the separation distance increases. The acceptable distance between platforms seems to vary depending on the platform and the location. Note that the two are usually convoluted so it is difficult to separate whether the difference is platform dependent or location dependent. For example, if a difference of 20 μmol mol^{-1} (10 $\times$ the ideal accuracy of the systems) were set as the limit for comparison (black dashed line in Fig. 6), the acceptable separation distance would range from only half a kilometer for the underway system to nearly 7 km for one of the moorings (vertical lines in Fig. 6, colors correspond with type of system comparison). Closer examination of the comparison data between the moorings at 47.967° and 47.327°N suggest daily variations in physical forcing (i.e., winds) drive the variability in correlation length scale rather than intrinsic site or instrument differences; however, all of these variables are extremely convoluted and difficult to isolate.

Despite the variations in correlation length scale, seawater xCO_2 comparisons between $ASVCO_2$ systems and other platforms were constrained to measurements taken within 20 min and 1 km of one another. The difference in the paired sea surface temperature (difference $<$ 0.5°C) and salinity (difference < 0.5) measurements from the onboard CTD confirmed the validity of these comparison constraints. Under these constraints, $ASVCO_2$ seawater xCO_2 measurements are in good agreement with concurrent measurements by other platforms, as seen in Fig. 5a (slope ≈ 1; $R^2 > 0.99$; RMSE < 5). One must be careful with fitting data like these with linear functions as the values at the extremes of the data range are disproportionately weighted, but these are encouraging results nonetheless. The mean differences between $ASVCO_2$ seawater xCO_2 measurements minus concurrent measurements (within 20 min and 1 km) made by moored $MAPCO_2$ systems, ship underway CO_2 systems, and another $ASVCO_2$ system equated to 1.2 ± 6.9 μmol mol^{-1}, -1.2 ± 3.0 μmol mol^{-1}, and -1.4 ± 3.4 μmol mol^{-1}, respectively (Table 1). Combined, these seawater xCO_2 comparisons show a mean difference of -0.5 ± 4.9 μmol mol^{-1} ($n = 250$). While the absolute mean difference for all seawater comparison data is similar to the atmospheric xCO_2 results (0.3 μmol mol^{-1}), the standard deviations are much higher than the atmospheric comparisons (2.0 μmol mol^{-1}). A portion of this variation is likely due to enhanced natural variability in seawater relative to air (Fig. 6).

These xCO_2 field intercomparison results are very similar to previous analysis of the $MAPCO_2$ technology that the $ASVCO_2$ is based on, and in this case, the statistics are more robust with 65% more seawater xCO_2 comparisons available for the $ASVCO_2$ than there were for the $MAPCO_2$ (Table 5 in Sutton et al. 2014). Laboratory testing of the $ASVCO_2$ system shows these systems have a precision of less than 0.7 μmol mol^{-1} and an accuracy of less than 1.5 μmol mol^{-1} for xCO_2 values between 100 and 600 μmol mol^{-1}. Other sources of error, such as the water vapor correction, results in a total uncertainty of calculated air and seawater pCO_2 of less

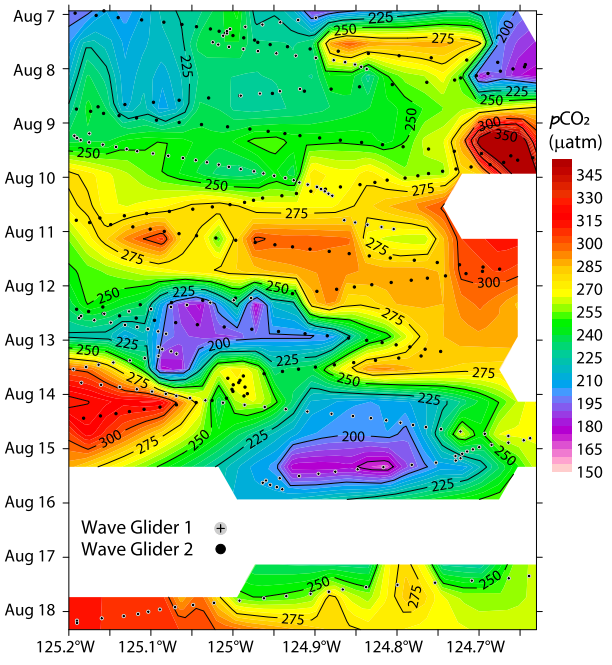

FIG. 7. Hovmöller diagram of surface seawater pCO_2 data (μatm) along the 47°N line in August 2011. Black and gray dots represent measurement locations.

than 2 μatm (Table 3 in Sutton et al. 2014). Given the laboratory testing results and the consistency of the resulting statistics for the $ASVCO_2$ comparisons with $MAPCO_2$ and shipboard underway systems, this suggests a similar air and seawater pCO_2 uncertainty of less than 2 μatm for the $ASVCO_2$ on Wave Glider and Saildrone platforms.

b. Design and operation

The goal of the $ASVCO_2$ development was to design a robust and accurate surface CO_2 system that could be used in a range of autonomous surface vehicles. The system has been tested on two very different platforms, the Wave Glider and the Saildrone. Each platform has a unique set of capabilities, but it can be useful to have the same instrumentation on these different platforms so that the data are comparable. The $ASVCO_2$ system is modified from the $MAPCO_2$ design, so very similar systems can now be deployed on fixed moorings and autonomous surface vehicles.

Each of the missions described here used the system in a different manner. In one deployment the system occupied a transect off the Washington coast for multiple days. This time series application of the platform-sensor combination is useful for demonstrating the variability of the area over time in more detail than a single mooring can provide (Fig. 7).

Figure 7 shows a Hovmöller diagram of surface seawater pCO_2 data along the 47°N line. This plot clearly shows the large variability observed during the survey period. The variability is driven by a dynamic interaction between high summertime productivity and coastal upwelling driven by upwelling-favorable winds during 8–12 August and again after 16 August. A ship-based survey aboard the R/V *Wecoma* sampled this line on 13 August, a period of relaxed winds that allowed the upwelling to subside and the local phytoplankton to draw down the surface pCO_2. These preliminary results show that the ship survey happened to sample during a period of low surface values. The $ASVCO_2$ systems on the Wave Gliders were able to characterize the conditions before and after the ship passed through to put that survey data in a temporal context.

The U.S. West Coast deployment of the Wave Gliders the following year, 2012, used a different approach to evaluate variability. Rather than focus on one transect, the two Wave Gliders were sent down the coast following the same path, but one Wave Glider was approximately 1 week behind the other. This approach characterized both spatial variability along the ASV track, but also temporal variability when comparing between the tracks of the two Wave Gliders (Fig. 8). This work clearly illustrates the temporal variability in pCO_2 resulting from changes in wind and upwelling regimes on time scales of a few days.

Although this manuscript has focused on the adaptation and evaluation of the $MAPCO_2$ for use on autonomous surface vehicles, these vehicles were also outfitted with a suite of other sensors (e.g., temperature, salinity, chlorophyll, dissolved oxygen, wind speed, and pH) that can provide a very rich context through which to interpret biogeochemical signals along the ASV track. For example, low salinity values (not shown) at 46°N indicate a plume of water from the Columbia River that resulted in low CO_2 values observed by both Wave Gliders (Fig. 8). Relatively cold sea surface temperatures confirmed a strong upwelling of high CO_2 waters at 42°N for the first Wave Glider, but had relaxed by the time the second Wave Glider passed through the area (Fig. 8). Measurements of pH using the Durafet sensors along these tracks provide a completely independent measurement and had a nearly identical pattern of variability to the CO_2. These measurements not only provide a useful check on the CO_2, but also provide the second parameter needed to evaluate ocean acidification along the West Coast.

The Saildrone is faster than the Wave Glider and can cover more ground. These vehicles have been used in a manner more similar to underway systems on research ships yet do not require a ship for deployment and recovery. Saildrones also have the advantage that they can transit into waters that are typically shallower than some large vessels are willing to enter. This potentially offers

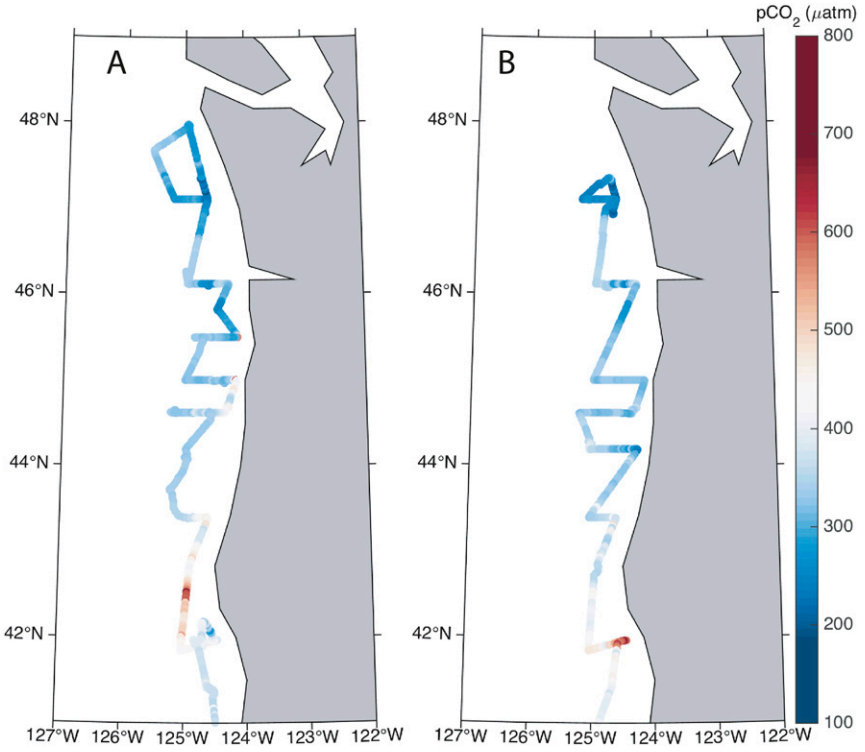

FIG. 8. Plots of surface seawater pCO_2 (μatm) along the U.S. West Coast (23 Aug–18 Oct 2012). Two Wave Gliders were deployed off Westport together. Both vehicles traveled north together for a day, and then (b) one vehicle was sent south to California. (a) The second Wave Glider went to 48°N and then turned south following behind the first Wave Glider on the same track about a week later.

the opportunity to map areas closer to the coast than one typically can get.

The viability of the Saildrone ASVCO_2 to make basin-scale surface pCO_2 observations was demonstrated during the 260-day mission from San Francisco Bay south to the Equator (Fig. 9). The ASVCO_2 observed a range of seawater pCO_2 of 350–550 μatm from the coastal shelf to the upwelling region of the tropical Pacific. In the equatorial region, the Saildrone crossed sharp fronts in seawater pCO_2 (e.g., Fig. 9 at 2°S, 125°W), SST, and SSS associated with tropical instability waves. While Saildrone navigation in low wind conditions was a challenge in this early mission to the tropical Pacific, subsequent ASV development has improved control under such conditions.

Thermodynamic and biological influences cause mesoscale temporal (from days to months) and spatial (km) variability in seawater carbon concentrations. Sparse measurements from instrumented survey expeditions and moorings can lead to biases in the characterization of these mesoscale dynamics within the carbon system, particularly in coastal regions. The new ASVCO_2 technology can be used to supplement current carbon measurement techniques, particularly with its cost-effective and energy-efficient design. The Wave Glider and Saildrone have the ability to accurately measure air–sea CO_2 with an overall uncertainty of ± 2 μatm paired with sea surface pH, SSS, and SST every 30 min. The short measurement interval provides carbon measurements that can capture small-scale spatiotemporal variability in the carbon system near the air–sea interface along the measurement

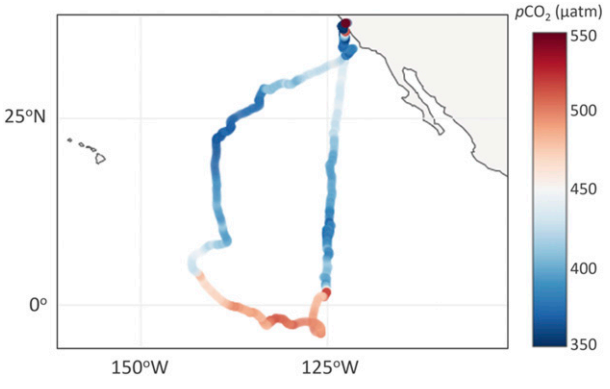

FIG. 9. Surface seawater pCO_2 (μatm) measured by a Saildrone ASVCO_2 during the 260-day mission to the tropical Pacific in 2017–18.

path. Wave Glider and Saildrone ASVCO_2 deployments combined with mooring and shipboard carbon measurements can contribute to a better understanding of past, present, and future carbon dynamics. In particular, with long transit capabilities and autonomous operation, Saildrone and Wave Glider ASVCO_2 systems have the potential to fill large observing gaps in the surface seawater pCO_2 network.

Acknowledgments. Primary support for this work was provided by the Office of Oceanic and Atmospheric Research of the NOAA, U.S. Department of Commerce, including resources from the Ocean Observing and Monitoring Division of the Climate Program Office (Fund Reference 100007298) and the Ocean Acidification Program, as well as NOAA's Hollings Undergraduate Scholarship and the Pacific Marine Environmental Laboratory. Additional funding from the Integrated Marine Observing System, and the Commonwealth Scientific and Industrial Research Organisation (CSIRO) supported the intercomparisons in Tasmanian waters. We gratefully acknowledge Todd Martz for supplying the Durafet electronic boards and firmware. We thank the crew of the R/V *Corliss*, R/V *Tatoosh*, R/V *Shimada*, and R/V *Investigator* and the Washington Department of Fisheries and Wildlife, the Olympic Coast National Marine Sanctuary, the National Marine Fisheries Service, and the CSIRO for accommodating deployments, recoveries, and intercomparisons for the ASVCO_2 systems. This is PMEL Contribution 5021 and SOEST Contribution 10986.

Data availability statement. Data presented in this paper are publicly available through the National Oceanic and Atmospheric Administration (NOAA) Ocean Carbon Data System repository located within the National Centers for Environmental Information (https://www.nodc.noaa.gov/ocads/).

REFERENCES

Bakker, D. C. E., and Coauthors, 2016: A multi-decade record of high-quality fCO_2 data in version 3 of the Surface Ocean CO_2 Atlas (SOCAT). *Earth Syst. Sci. Data*, **8**, 383–413, https://doi.org/10.5194/essd-8-383-2016.

Barton, A., B. Hales, G. G. Waldbusser, C. Langdon, and R. A. Feely, 2012: The Pacific oyster, *Crassostrea gigas*, shows negative correlation to naturally elevated carbon dioxide levels: Implications for near-term ocean acidification effects. *Limnol. Oceanogr.*, **57**, 698–710, https://doi.org/10.4319/lo.2012.57.3.0698.

Bates, N. R., and Coauthors, 2014: A time-series view of changing ocean chemistry due to ocean uptake of anthropogenic CO_2 and ocean acidification. *Oceanography*, **27** (1), 126–141, https://doi.org/10.5670/oceanog.2014.16.

Bauer, J. E., W.-J. Cai, P. A. Raymond, T. S. Bianchi, C. S. Hopkinson, and P. A. G. Regnier, 2013: The changing carbon cycle of the coastal ocean. *Nature*, **504**, 61–70, https://doi.org/10.1038/nature12857.

Bednaršek, N., G. A. Tarling, S. Fielding, and D. C. E. Bakker, 2012: Population dynamics and biogeochemical significance of *Limacina helicina antarctica* in the Scotia Sea (Southern Ocean). *Deep-Sea Res. II*, **59–60**, 105–116, https://doi.org/10.1016/j.dsr2.2011.08.003.

——, ——, D. C. E. Bakker, S. Fielding, and R. A. Feely, 2014a: Dissolution dominating calcification process in polar pteropods close to the point of aragonite undersaturation. *PLOS ONE*, **9**, e109183, https://doi.org/10.1371/journal.pone.0109183.

——, R. A. Feely, J. C. P. Reum, B. Peterson, J. Menkel, S. R. Alin, and B. Hales, 2014b: *Limacina helicina* shell dissolution as an indicator of declining habitat suitability owing to ocean acidification in the California Current ecosystem. *Proc. Roy. Soc.*, **281B**, 20140123, https://doi.org/10.1098/RSPB.2014.0123.

——, T. Klinger, C. J. Harvey, S. Weisberg, R. M. McCabe, R. A. Feely, J. Newton, and N. Tolimieri, 2017: New ocean, new needs: Application of pteropod shell dissolution as a biological indicator for marine resource management. *Ecol. Indic.*, **76**, 240–244, https://doi.org/10.1016/j.ecolind.2017.01.025.

Bresnahan, P. J., T. R. Martz, Y. Takeshita, K. S. Johnson, and M. LaShomb, 2014: Best practices for autonomous measurement of seawater pH with the Honeywell Durafet. *Methods Oceanogr.*, **9**, 44–60, https://doi.org/10.1016/j.mio.2014.08.003.

Chavez, F. P., J. Sevadjian, C. Wahl, J. Friederich, and G. E. Friederich, 2018: Measurements of pCO_2 and pH from an autonomous surface vehicle in a coastal upwelling system. *Deep-Sea Res. II*, **151**, 137–146, https://doi.org/10.1016/j.dsr2.2017.01.001.

Damm, E., E. Helmke, S. Thoms, U. Schauer, E. Nöthig, K. Bakker, and R. P. Kiene, 2010: Methane production in aerobic oligotrophic surface water in the central Arctic Ocean. *Biogeosciences*, **7**, 1099–1108, https://doi.org/10.5194/bg-7-1099-2010.

Dlugokencky, E. J., J. W. Mund, A. M. Crotwell, M. J. Crotwell, and K. W. Thoning, 2016: Atmospheric carbon dioxide dry air mole fractions from the NOAA ESRL carbon cycle cooperative global air sampling network, 1968–2016, version 2017-07. NOAA, accessed 1 August 2017.

——, K. W. Thoning, P. M. Lang, and P. P. Tans, 2019: NOAA greenhouse gas reference from atmospheric carbon dioxide dry air mole fractions from the NOAA ESRL carbon cycle cooperative global air sampling network. NOAA, accessed 10 January 2020, ftp://aftp.cmdl.noaa.gov/data/trace_gases/co2/flask/surface/.

Fabry, V. J., B. A. Seibel, R. A. Feely, and J. C. Orr, 2008: Impacts of ocean acidification on marine fauna and ecosystem processes. *ICES J. Mar. Sci.*, **65**, 414–432, https://doi.org/10.1093/icesjms/fsn048.

Fassbender, A. J., and Coauthors, 2018: Seasonal carbonate chemistry variability in marine surface waters of the US Pacific Northwest. *Earth Syst. Sci. Data*, **10**, 1367–1401, https://doi.org/10.5194/essd-10-1367-2018.

Feely, R. A., and Coauthors, 2016: Chemical and biological impacts of ocean acidification along the west coast of North America. *Estuarine Coastal Shelf Sci.*, **183**, 260–270, https://doi.org/10.1016/J.ECSS.2016.08.043.

Friedlingstein, P., and Coauthors, 2019: Global carbon budget 2019. *Earth Syst. Sci. Data*, **11**, 1783–1838, https://doi.org/10.5194/essd-11-1783-2019.

Gruber, N., and Coauthors, 2019: The oceanic sink for anthropogenic CO_2 from 1994 to 2007. *Science*, **363**, 1193–1199, https://doi.org/10.1126/science.aau5153.

Humphries, R. S., I. M. McRobert, W. A. Ponsonby, J. P. Ward, M. D. Keywood, Z. Loh, P. B. Krummel, and J. Harnwell, 2019:

Identification of platform exhaust on the RV Investigator. *Atmos. Meas. Tech.*, **12**, 3019–3038, https://doi.org/10.5194/amt-12-3019-2019.

Keeling, C. D., S. C. Piper, R. B. Bacastow, M. Wahlen, T. P. Whorf, M. Heimann, and H. A. Meijer, 2005: Atmospheric CO_2 and $^{13}CO_2$ exchange with the terrestrial biosphere and oceans from 1978 to 2000: Observations and carbon cycle implications. *A History of Atmospheric CO_2 and Its Effects on Plants, Animals, and Ecosystems*, I. T. Baldwin et al., Eds., Springer, 83–113.

Kleypas, J. A., R. A. Feely, V. J. Fabry, C. Langdon, C. L. Sabine, and L. L. Robbins, 2006: Impacts of ocean acidification on coral reefs and other marine calcifiers: A guide for future research. NSF–NOAA–USGS Rep., 88 pp.

Landschützer, P., N. Gruber, D. C. E. Bakker, and U. Schuster, 2014: Recent variability of the global ocean carbon sink. *Global Biogeochem. Cycles*, **28**, 927–949, https://doi.org/10.1002/2014GB004853.

Lindquist, A., and Coauthors, 2018: Puget Sound marine waters: 2017 overview. NOAA Rep., 52 pp., https://www.psp.wa.gov/PSmarinewatersoverview.php.

Martz, T. R., J. G. Connery, and K. S. Johnson, 2010: Testing the Honeywell Durafet® for seawater pH applications. *Limnol. Oceanogr. Methods*, **8**, 172–184, https://doi.org/10.4319/lom.2010.8.172.

Meinig, C., R. Jenkins, N. Lawrence-Slavas, and H. Tabisola, 2015: The use of Saildrones to examine spring conditions in the Bering Sea: Vehicle specification and mission performance. *OCEANS 2015*, Washington, DC, Marine Technology Society–IEEE, https://doi.org/10.23919/OCEANS.2015.7404348.

——, and Coauthors, 2019: Public–private partnerships to advance regional ocean-observing capabilities: A Saildrone and NOAA-PMEL case study and future considerations to expand to global scale observing. *Front. Mar. Sci.*, **6**, 448, https://doi.org/10.3389/FMARS.2019.00448.

Northcott, D., J. Sevadjian, D. A. Sancho-Gallegos, C. Wahl, J. Friederich, and F. P. Chavez, 2019: Impacts of urban carbon dioxide emissions on sea-air flux and ocean acidification in nearshore waters. *PLOS ONE*, **14**, e0214403, https://doi.org/10.1371/journal.pone.0214403.

Olsen, A., and Coauthors, 2019: GLODAPv2.2019—An update of GLODAPv2. *Earth Syst. Sci. Data*, **11**, 1437–1461, https://doi.org/10.5194/essd-11-1437-2019.

Pierrot, D., and Coauthors, 2009: Recommendations for autonomous underway pCO_2 measuring systems and data-reduction routines. *Deep-Sea Res. II*, **56**, 512–522, https://doi.org/10.1016/j.dsr2.2008.12.005.

Reum, J. C. P., and Coauthors, 2015: Interpretation and design of ocean acidification experiments in upwelling systems in the context of carbonate chemistry co-variation with temperature and oxygen. *ICES J. Mar. Sci.*, **73**, 582–595, https://doi.org/10.1093/ICESJMS/FSU231.

Sabine, C. L., and Coauthors, 2004: The oceanic sink for anthropogenic CO_2. *Science*, **305**, 367–371, https://doi.org/10.1126/science.1097403.

Sutton, A. J., and Coauthors, 2014: A high-frequency atmospheric and seawater pCO_2 data set from 14 open-ocean sites using a moored autonomous system. *Earth Syst. Sci. Data*, **6**, 353–366, https://doi.org/10.5194/essd-6-353-2014.

——, and Coauthors, 2019: Autonomous seawater pCO_2 and pH time series from 40 surface buoys and the emergence of anthropogenic trends. *Earth Syst. Sci. Data*, **11**, 421–439, https://doi.org/10.5194/essd-11-421-2019.

Takahashi, T., and Coauthors, 2009: Climatological mean and decadal change in surface ocean pCO_2, and net sea-air CO_2 flux over the global oceans. *Deep-Sea Res. II*, **56**, 554–577, https://doi.org/10.1016/j.dsr2.2008.12.009.

Wanninkhof, R., R. Feely, A. Sutton, C. Sabine, K. Tedesco, N. Gruber, and S. Doney, 2013a: An integrated ocean carbon observing system (IOCOS). *U.S. IOOS Summit*, Herndon, VA, Interagency Ocean Observation Committee.

——, and Coauthors, 2013b: Global ocean carbon uptake: Magnitude, variability and trends. *Biogeosciences*, **10**, 1983–2000, https://doi.org/10.5194/BG-10-1983-2013.

——, L. Barbero, R. Byrne, W.-J. Cai, W.-J. Huang, J.-Z. Zhang, M. Baringer, and C. Langdon, 2015: Ocean acidification along the Gulf Coast and east coast of the USA. *Cont. Shelf Res.*, **98**, 54–71, https://doi.org/10.1016/j.csr.2015.02.008.

Willcox, S., C. Meinig, C. L. Sabine, N. Lawrence-Slavas, T. Richardson, R. Hine, and J. Manley, 2010: An autonomous mobile platform for underway surface carbon measurements in open-ocean and coastal waters. *OCEANS 2009*, Biloxi, MS, Marine Technology Society–IEEE, https://doi.org/10.23919/OCEANS.2009.5422067.